Gómez-de Pedro, S., Salinas-Castillo, A., Ariza-Avidad, M., Lapresta-Fernández, A., Sánchez-González, C., Martínez-Cisneros, C.S., Puyol, M., Capitan-Vallvey, L.F., Alonso-Chamarro, J. (2014). Microsystem-assisted synthesis of carbon dots with fluorescent and colorimetric properties for pH detection. *Nanoscale*, 6, pp. 6018-6024.

Microsystem-assisted synthesis of carbon dots with fluorescent and colorimetric properties for pH detection

S. Gómez-de Pedro,[a] A. Salinas-Castillo,*[b] M. Ariza-Avidad,[b] A. Lapresta-Fernández,[b] C. Sánchez-González,[c] C. S. Martínez-Cisneros,[a] M. Puyol,[a] L. F. Capitan-Vallvey[b] and J. Alonso-Chamarro[a]

The present paper describes the use of a microfluidic system to synthesize carbon dots (Cdots) and their use as optical pH sensors. The synthesis is based on the thermal decomposition of ascorbic acid in dimethyl sulfoxide. The proposed microsystem is composed of a fluidic and a thermal platform, which enable proper control of synthesis variables. Uniform and monodispersed 3.3 nm-sized Cdots have been synthesized, the optical characterization of which showed their down/upconversion luminescence and colorimetric properties. The obtained Cdots have been used for pH detection with down and upconverison fluorescent properties as excitation sources. The naked eye or a photographic digital camera has also been implemented as detection systems with the hue parameter showing a linear pH range from 3.5 to 10.2. On the other hand, experiments on the cytotoxicity and permeability of the Cdots on human embryonic kidney cells revealed their adsorption on cells without causing any impact on the cellular morphology.

1. Introduction

The recent application of fluorescent nanoparticles (NPs) such as quantum dots, dye-doped NPs and rare earth-based NPs in biomedical sensing and imaging has become a major subject of research over the last few years. Although a wide range of diverse photoluminescent NPs have been developed from new materials, an increased concern about their potential environmental and human health toxicity exists.[1] Moreover, there are some NP-associated drawbacks such as modification of their surface for a particular function which involves highly time-consuming processes.

At the moment, one of the most attractive NPs are carbon dots (Cdots), which have recently had a major relevance in analytical and bioanalytical chemistry mainly due to their excellent luminescent properties and high biocompatibility as well as their low cost synthesis.[2] However, although these Cdots are very promising NPs in nanotechnology and nano-biomedicine, much research needs to be done either to investigate their potential in sensor development or to identify novel synthesis approaches. In addition, Cdots show size dependent photoluminescence and upconversion luminescence properties leading to anti-Stokes type emissions.[3]

Many different approaches have been presented to date to synthesize Cdots. They are based on two routes, top-down and bottom-up methods. The top-down methods synthesize Cdots from larger carbon materials (graphite, carbon nanotubes, carbon soots, activated carbon), using arc discharge, laser ablation or electrochemical oxidation.[4] The bottom-up routes synthesize Cdots from molecular precursors by combustion, thermal decomposition, acid dehydration, ultrasonic or microwave pyrolysis.[5] However, most of these synthetic approaches present poor reproducibility, which leads to the formation of Cdots with different optical and electronic properties in the different batches produced.

In this sense, microfluidic systems can offer some advantages when synthesizing nanoparticles. They permit proper control of some critical synthesis variables such as the mass and temperature transference due to the small dimensions of the fluidic channels, which are, in contrast, difficult to manage in conventional methods. Moreover, the addition of reagents can be computer-controlled, which permits varying as desired flow rates or injection volumes to obtain products of reactions of different characteristics as well as conferring safety to the operator. On the other hand, the easy and fast modification of the hydrodynamic parameters permits performing many different reactions in a short time, which considerably simplifies the optimization process for the synthesis of

[a]Sensors & Biosensors Group, Departament of Chemistry, Auntonomus University, Edifici Cn., 08193 Bellatera, Catalonia, Spain

[b]ECsens, Department of Analytical Chemistry, Faculty of Sciences, University of Granada, E-18071 Granada, Spain. E-mail: alfonsos@ugr.es; Fax: +34 958 243 328; Tel: +34 958 248 436

[c]Department of Physiology, School of Pharmacy, University of Granada, Granada 18071, Spain

nanomaterials. All this leads to the production of uniform and well dispersed colloids in a reproducible way, namely with the same electronic, optical and chemical properties, which is of great importance for the application of nanomaterials in the (bio)analytical field. Proof of all the advantages enumerated is the large number of papers devoted to that in the literature.[6]

Ceramic microfluidic systems have shown great potential in the synthesis of nanoparticles.[7] This material and its associated technology (Low-Temperature Co-fired Ceramics technology (LTCC)) allow the integration of diverse electronic or fluidic components in a simple, low cost and rapid way. Its multilayer approach enables easy construction of three-dimensional structures, and its compatibility with screen-printing techniques permits integration of many electronic components, such as detection or heating systems.[8,9]

Herein, we synthesize Cdots in a microfluidic system composed of two modules, one for microfluidics and another for heating and temperature control. A proper optimization of the chemical and hydrodynamic parameters has been performed in order to obtain stable and well-dispersed Cdots. As far as we are aware, no microfluidic approach has yet been reported for synthesizing Cdots.

The optical properties of the obtained Cdots have been used for the development of a fluorescent sensor for pH detection using UV and NIR excitation sources. Additionally, due to color changes of Cdots, the visual detection of pH was possible by using digital camera photography and the hue (H) parameter.

Finally, the cytotoxicity and permeability of the NPs in human embryonic kidney cells have also been studied to demonstrate their suitability as sensors or labels in biomedical applications by bioimaging.

2.   Experimental

Microsystem materials and components

DuPont 951 green tape (DupontTM, Germany) was used to fabricate both the microfluidic and the heating modules. DuPont 5742 gold cofirable conductor paste was required in order to perform the screen-printing step for the construction of the heating platform, since the gold paste acts as the resistor. DuPont 6141 paste was used to fill the vials of the heating platform. For temperature control, a class A PT100 temperature sensor was preferred (Innovative Sensor Technology, Switzerland). The sensor was glued to the bottom of the heating module by means of epoxy (EPO-TEK® H20E, Billerica, MA, USA), and a PIC18F4431 microcontroller (Microchip Inc., Arizona, USA) was used for the digital PID control system, which controls the temperature as desired.

In the flow system, a 10 mL syringe (Hamilton series GASTIGHT 1000 TLL, Bonaduz, GR, Switzerland) was required, where reagents were placed for their injection into the microfluidic system by means of a syringe pump (540 060 TSE systems, Bad Homburg, Germany). To complete the fluidic system, PTFE tubes (i.d. 0.9 mm) were used between the syringe and the microfluidic platform, and o-rings and conic PTFE cones were used for their connection.

Instrumentation

Optical properties of the nanoparticles were obtained by means of Varian Cary Eclipse (Varian Ibérica, Madrid, Spain) and Fluorolog1 Modular (Horiba Jobin Yvon, France) spectrofluorometers. Zeta-potential measurement was carried out on a Zetasizer Nano ZS90 (Malvern, Worcestershire, U.K.). XRD was performed at the Centre of Scientific Instrumentation (University of Granada, Spain) on a Fisons-Carlo Erba analyser model EA 1108. The FTIR spectra of the powdered samples were recorded with a ThermoNicolet IR200FTIR (Thermo Fisher Scientific Inc., Madrid, Spain) by using KBr pellets.

The shape and dimensions of the core of the particles were measured using a high resolution electron microscope (HRTEM), JEOL 2011 (Tokyo, Japan). The samples were prepared by dipping a copper grid, which was coated with a thin carbon film, into the carbon dot suspension.

A Crison pH meter (Crison Instruments, Barcelona, Spain, model Basic 20) was used for pH measurements.

pH measurement procedure

The pH of 2 mL of Cdot solutions was regulated by adding different volumes of required concentrations of HCl or NaOH and measuring it with a pH meter. The fluorescence spectra and the image capture with a digital camera were recorded at different pH values.

Image acquisition and treatment for colorimetric pH determination

For image acquisition and digitization, a Canon PowerShot G12 (Madrid, Spain) was used. To keep all the image-gathering under the same conditions a Cube Light Box was developed. The vials with 2 mL of Cdots were located inside the box, so they were not exposed to external light. The only light source was an LED (Light-Emitting Diode) system with direct current. All parameters of the camera were set and optimized. The vial position was fixed for all experiments.

The obtained images were stored in the TIFF (True Image File Format) file format to prevent any loss of information since it does not compress the image. To extract the hue parameter from each sensing element in the scanned image, software developed by the research group in Matlab was used. The H coordinate was calculated from the R, G and B coordinates of each pixel using eqn (1). The H value, determined for each sensing element, was the mode of the hues calculated for all the pixels in the solution, since this parameter provides low error during image processing.

$$
\begin{aligned}
H = &\left(\frac{G - B}{\max_{\text{channel}} - \min_{\text{channel}}} + 0\right)\Big/6; \quad \text{if } \max = R* \\
&\left(\frac{B - R}{\max_{\text{channel}} - \min_{\text{channel}}} + 2\right)\Big/6; \quad \text{if } \max = G \qquad (1) \\
&\left(\frac{R - G}{\max_{\text{channel}} - \min_{\text{channel}}} + 4\right)\Big/6; \quad \text{if } \max = B
\end{aligned}
$$

* if H is less than 0 then add 1 to H.

Cell culture

Human embryonic kidney HEK293 cells were cultured in Dulbecco's modified Eagle's medium (DMEM) supplemented with 10% fetal bovine serum, 2 mM L-glutamine and 1% penicillin–streptomycin solution at 37 °C with 5% humidified CO_2. Cells were plated at 20 000 cells per well onto glass bottom Petri dishes previously coated with 10 g mL^{-1} poly-L-lysine. After 24 h in culture, the cells were incubated for 24 or 48 h at 37 °C with different concentrations of Cdots (0.1, 0.2, 0.4, 0.6, 0.8, 1 mg mL^{-1}) dispersed in complete culture medium.

Cytotoxicity assay

In vitro proliferation assay compared the growth rate of HEK293 cells using 3-(4,5-dimethyl-1,3-thiazol-2-yl)-2,5-diphenyl-2*H*-tetrazol-3-ium bromide (MTT) after plating 2×10^4 cells per well on a 96-well flat-bottom plate for 24 and 48 h at 37 °C in 5% CO_2. MTT (5 mg mL^{-1}) reagent was added to each well and incubated for 4 h at 37 °C. Thereafter, 150 mL per well of 100% DMSO were added, mixed thoroughly to dissolve the dark blue crystals and the plates were subsequently read on an ELISA reader at a wavelength of 570 nm.

Fluorescence microscopy

Fluorescence measurements were performed with a Zeiss (Oberkochen, Germany) Axiovert 200 inverted microscope fitted with an ORCA-ER CCD camera (Hamamatsu, Bridgewater, NJ) through a 20× air objective. Nanoparticles were excited at 360/380 nm using a computer-controlled Lambda10-2 filter wheel (Sutter Instruments, Novato, CA), and emitted fluorescence was filtered with a 440/535 nm long-pass filter. Images were processed with Image J software.

3. Results and discussion

3.1 Design and fabrication of the microsystem

The microsystem for the synthesis of Cdots was based on two separate modules: a microfluidic platform and a heating module with temperature control. The general fabrication procedure of ceramic microsystems is detailed elsewhere.[10] Since the LTCC technology is a multilayer approach, the final design of the device has to be divided into different layers in order to create the partial design by means of computer-assisted design (CAD) software. In this step, it has to be taken into account the ~15% shrinkage on each axis of DuPont 951 green tape during the sintering process. Once the design is done, a laser machine (LPKF Protolaser 200, Garbsen, Germany) transfers the diverse patterns to different layers. The next step in the construction of the device involves screen-printing of those layers that require conductive paste. In this case, this step was necessary in the layers which formed the heating platform (resistor and vias to connect the tracks). The heater was constructed in the base of a gold paste screen-printed resistor, which was deposited in a radial configuration. Then, the slabs were aligned in aluminium plates using fiducial holes and laminated by a thermo-compression process at 100 °C and 3000 psi. The LTCC layers were finally sintered in a programmable box furnace (Carbolite CBCWF11/23P16, Afora, Barcelona, Spain) by applying a temperature profile.

As explained before, two different modules were preferred to carry out the synthesis of carbon dots, which were mechanically attached to obtain the best contact between them. In this way, if one of the modules has to be modified, it can be replaced without changing the other one. Both modules were designed and constructed based on a previous microsystem.[9]

The fluidic platform had one inlet for the entrance of reagents followed by a simple Z shape channel to increase the residence time of reagents inside the microsystem and allow their thermal conditioning, and one outlet from which the formed Cdots leave the system. The Z-shape fluidic structure was constructed in a circular configuration in order to make it coincide with the resistance of the heating module. Moreover, the channel for reagents was constructed in only one layer of the ceramic substrate, since deeper channels could generate no uniform thermal patterns through the solution. All this contributes to obtaining well controlled heat transfer from the thermal platform to the liquid flowing in the microfluidic platform, which ensures the optimal and uniform formation of carbon dots through the microsystem.[11] As can be observed in Fig. 1, the whole module consisted of 7 ceramic layers, which once sintered formed a block of 6.0 mm diameter and 1.4 mm thickness. An image of the different layers that compose both the fluidic and the heating platforms is depicted in Fig. 1.

To make proper control of the temperature feasible, a class A PT100 sensor was attached by means of epoxy on the reverse of the bottom layer, taking care of the position of the sensor in the central zone of the resistor. Electronics for temperature control is detailed elsewhere.[9] Briefly, a temperature controller with a digital PID topology was implemented on a computer controlled PIC18F4431 microcontroller. An electronic circuit maintained a constant intensity in order to avoid interference with temperature measurements due to self-heating, and amplified the control signal generated by the PID controller. The system estimated the error from the PT100 sensor through the obtained feedback signal and corrected it by specific differential equations programmed in the digital PID control system implemented in the microcontroller code. Then, the signal was amplified and applied to the gold resistor. The system was programmed to work from 150 to 250 °C.

Heat transfer in the thermal platform exhibited a radial distribution, and it was found to provide the temperature desired in the fluidic system, since the sensor is located trying to obtain the optimum *xy*-alignment with the microreactor zone.[11]

3.2 Synthesis of Cdots

For the synthesis of Cdots, ascorbic acid (Panreac, 99%) was chosen as a simple and low cost source of carbon, and dimethyl sulfoxide (DMSO) (Baker Chemical, 0.3% water) was preferred as solvent due to the high temperatures that this compound can bear.

In order to obtain controllable and reproducible carbon dots, optimization of certain parameters of the microsystem is
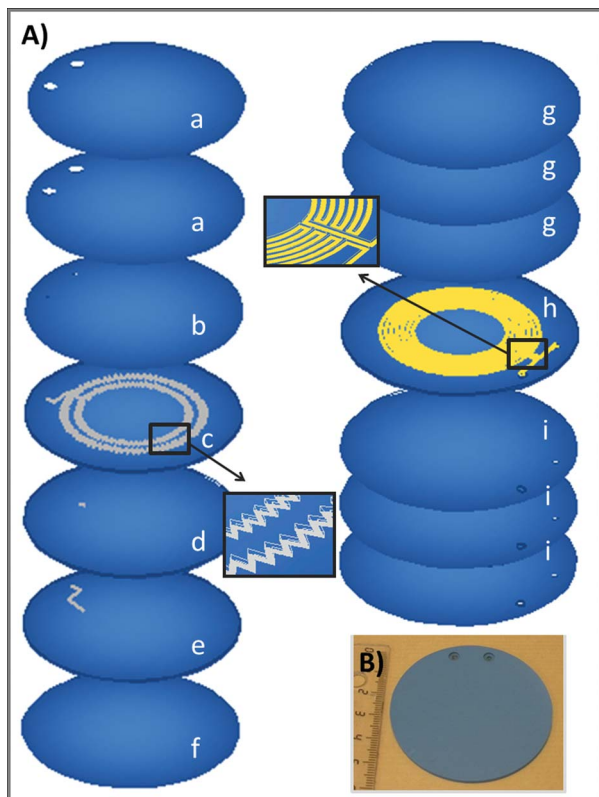
Fig. 1 (A) Scheme of the different layers that compose the microfluidic system for the synthesis of carbon dots. Layers (a–f) correspond to the microfluidic platform: (a) top layers, where o-rings are placed; (b) entrance and exit for reagents and the product; (c) inlet for reagents and the bidimensional micromixer; (d) intermediate layer for the connexion of the fluidic structure; (e) outlet for the synthesized carbon dots; (f) bottom layer. Layers (g–i) compose the thermal platform: (g) top layers; (h) embedded screen-printed heater; (i) bottom layers with vias to connect the tracks of the resistance. (B) Picture of both the microfluidic and the heating platforms mechanically attached.

Fig. 2 Optimization of the chemical and hydrodynamic parameters for the synthesis of Cdots in the ceramic microfluidic system (λ_{exc} = 325 nm, λ_{em} = 420 nm). Red circles: temperature (°C), blue squares: concentration ($\mu g\ mL^{-1}$), green triangles: flow rate ($\mu L\ min^{-1}$).

required. The optimized values were determined as a function of the maximum fluorescence intensity recorded with a spectrofluorometer, since the synthesized Cdots are designed to use for sensing and bioimaging applications.

As in many other nanoparticle syntheses that involve the decomposition of reagents, temperature plays an important role. Thus, the first parameter to study was the reaction temperature. Since ascorbic acid has a melting point of 188 °C, six different temperatures around this value (180, 190, 195, 200, 210 and 240 °C) were chosen. The concentration of ascorbic acid and the flow rate were fixed to 0.1 mg mL^{-1} and 20 μL min^{-1}, respectively. As can be observed in Fig. 2, only a weak fluorescence intensity was observed from the Cdots synthesized at 180 °C, which indicates the poor formation of the nanoparticles at temperatures below the ascorbic acid melting point. A clear improvement is observed when performing the reaction under the same conditions but by increasing the temperature over this threshold. On the other hand, from 190 °C up to 240 °C the fluorescence intensity remained practically constant. The small decrease observed is probably due to the decomposition of the
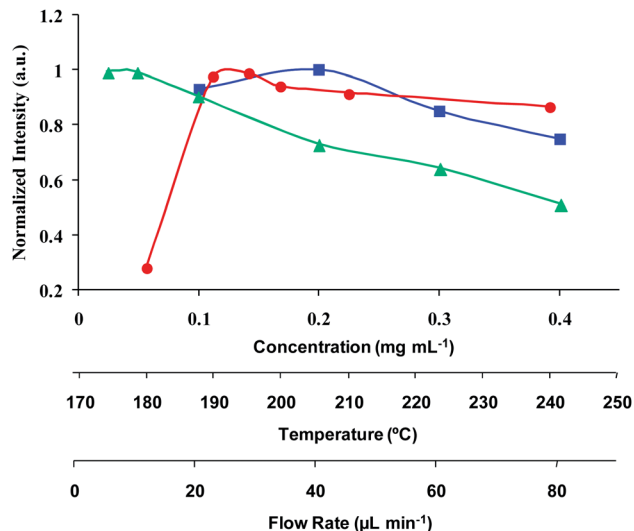
solvent (boiling point of 189 °C), which generates gaseous species such as SO$_2$.[12] Thus, 190 °C was preferred as the optimized value for temperature to perform the synthesis. All the fluorescence emission spectra of the Cdots synthesized exhibit the same maximum peak, located over 420 nm.

The effect of varying the concentration of ascorbic acid was also studied. Four different concentrations were evaluated (0.1, 0.2, 0.3 and 0.4 mg mL^{-1}), while temperature was fixed at 190 °C and flow rate at 20 μL min^{-1}. As shown in Fig. 2, the concentration at which higher intensity of fluorescence was observed under these conditions was 0.2 mg mL^{-1}, and thus, this value was selected for further optimization.

Finally, the variation in the flow rate of reagents in the microfluidic system was evaluated, while the remaining parameters were fixed at the optimized conditions (a temperature of 190 °C and an ascorbic acid concentration of 0.2 mg mL^{-1}). The tested values included 5, 10, 20, 40, 60 and 80 μL min^{-1}. As presented in Fig. 2, the more slowly the liquid flowed in the system, the higher fluorescence was achieved. This was in concordance with the fact that the time that reagents spend in the microfluidic system determines the reaction time for the formation of colloids. This is a critical variable,[13] and, in this work, 10 μL min^{-1} (instead of 5 μL min^{-1}) was selected as a compromise between the intensity of fluorescence and the final amount of the colloid obtained in a reasonable synthesis time.

3.3 Characterization of Cdots

Cdots synthesized in the microsystem were dialyzed against Milli-Q water using spectra/pro-dialysis membrane with a cut-off of 1 kDa for their purification and characterized by several techniques.

The core and shape of the nanoparticles were determined by Transmission Electron Microscopy (TEM). Fig. 3A shows a TEM image, where monodispersed spherical carbon dots can be
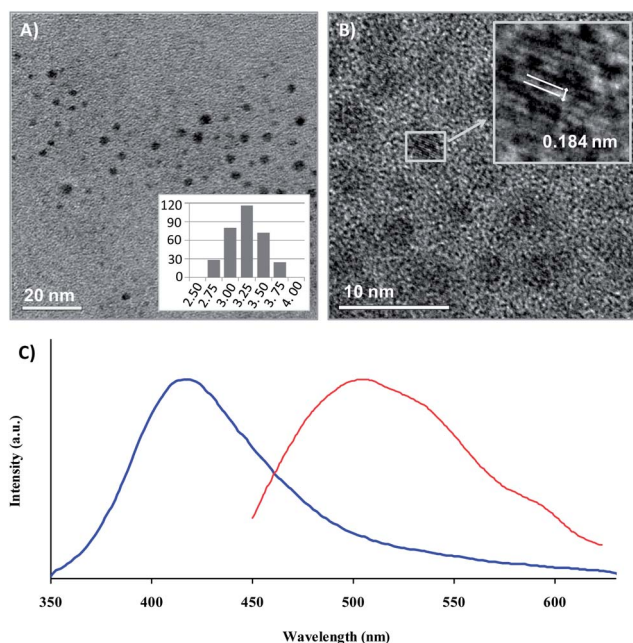
Fig. 3 Characterization of the synthesized Cdots in the microfluidic system. (A) TEM image with the size-histogram and the calculated average size. (B) HRTEM image and an amplification with the lattice fringes highlighted. (C) Fluorescence emission spectrum by UV excitation at 325 nm (in blue) and by NIR excitation at 850 nm (in red).

observed. The average size found was 3.3 ± 0.3 nm from the counting of more than 250 particles, which demonstrates the synthesis reproducibility of the microsystem. HRTEM (High-Resolution Transmission Electron Microscopy) images (Fig. 3B) revealed crystalline nanoparticles, as was also proved by the clear ring structure of the selected area electron diffraction (SAED) pattern image. Lattice planes with 0.18 nm spacing were found in the crystalline images from the colloid, which is consistent with the (102) diffraction planes of sp^2 graphitic carbon.[14] The bright rings observed in the SAED pattern can be attributed to (100) and (102) lattice planes of graphite (inset of Fig. 3B).

The FTIR spectrum of Cdots showed the typical bands of stretching vibrations of O–H at 3400 cm^{-1}, the ester group at 1780 cm^{-1} and C=O at 1622 cm^{-1}. The X-ray diffraction (XRD) pattern displayed a broad diffraction peak at $2\Phi = 20.5°$. Different zeta potential values were obtained for the synthesized Cdots, varying from acid pH (8 mV) to basic pH (−14 mV), which confirms the presence of carboxyl groups on the surface of the nanoparticles.

Cdots exhibited excellent water solubility and blue luminescence under UV excitation light (365 nm). Using quinine sulphate as standard, the fluorescence quantum yield was found to be 2.6%, which is comparable to previous reports.

To further explore the optical properties of Cdots, a detailed fluorescence study was performed using different excitation wavelengths (Fig. 3C). It is remarkable that these Cdots also exhibit good upconversion fluorescent properties besides their strong luminescence in the visible region under NIR excitation sources. Fig. 3C shows the fluorescent spectra of Cdots excited

at 325 nm with emission in the range of 360–500 nm (see Fig. 3C blue), and excited by longer wavelength light (maximum intensity with 850 nm excitation, see Fig. 3C red) with the up-conversion emissions located in the range of 450–600 nm. Therefore, these results suggest that Cdots may be used as a powerful component in biological applications as well as an appropriate sensor design for environmental applications.

3.4 Sensing applications

It is already known that Cdots are pH sensitive. Indeed, diverse studies can be found in the literature which describe the sensitivity of Cdots to pH depending on their external composition (carbonyls, amines, hydroxyls, esters, *etc.*). In particular, a previous study showed that Cdots synthesized from ascorbic acid pyrolysis were capable of detecting small pH changes by colorimetry or fluorimetry.[5c] That is, the intensity of fluorescence change with protonation and deprotonation of the carboxyl groups of the surface Cdots cause electrostatic doping/ charging of the Cdots and shift the Fermi level. Similarly, the
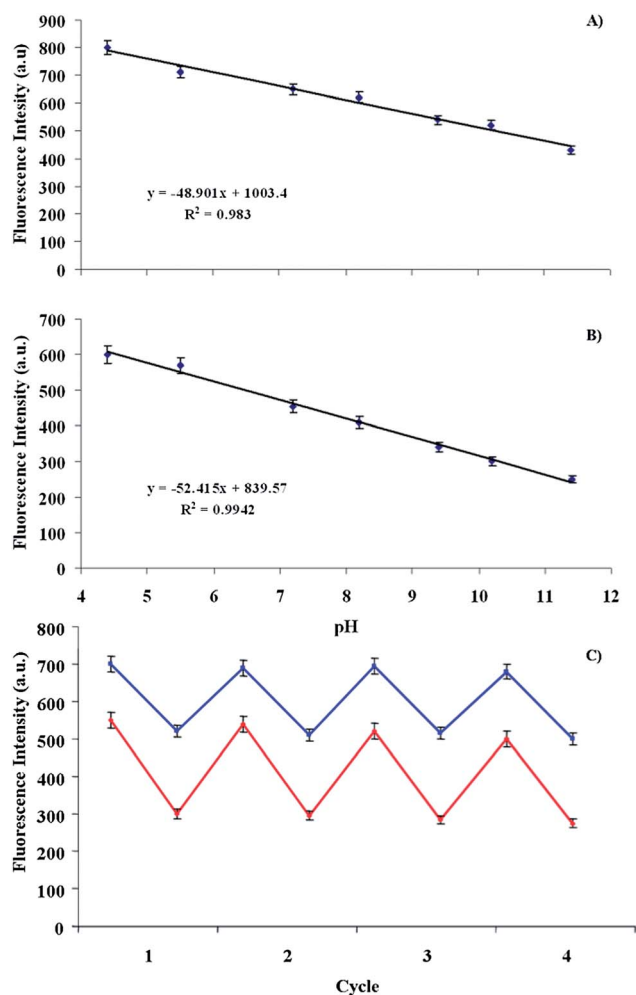

Fig. 4 Linear calibration plots for pH detection are shown in (A) for fluorescence (λ_{exc} = 325 nm, λ_{ems} = 420 nm) and (B) for up-conversion fluorescence (λ_{exc} = 850 nm, λ_{ems} = 505 nm). (C) Plots of the fluorescence intensity as a function of pH cycles ($\lambda_{exc/ems}$ = 325/420 nm blue), ($\lambda_{exc/ems}$ = 850/505 nm red).

color of the Cdot solution change with pH causes electronic changes of π–π* and n–π* by refilling or depleting their valence bands.[15]

Since the obtained Cdots have the same matrix, it is expected that they have the same behavior and therefore, one can take advantage of this fact to advance their application as pH sensors.

Fluorescent sensor for pH. The influence of pH on the synthesized Cdots in the pH range of 2–11 was studied. The results showed that the maximum fluorescence emission (420 nm) of the Cdots at 325 nm excitation decreased linearly as the pH increased from 4.5–11.5 (Fig. 4A), and the same results were obtained by excitation at 850 nm and emission at 505 nm (Fig. 4B).

The good emission fluorescence presented at 400 or 505 nm by the Cdots over a wide range of pH (4.5–11.5) makes them valuable for future use in biological applications.

In order to test the reversibility of the proposed nanosensor, the pH of Cdots was changed from 5 to 10 and back to 5 four times, and the fluorescence was measured by down and upconverting excitation emission values in all cases. The results confirmed the good reversibility of the nanosensor (see Fig. 4C). The relative standard deviations were less than 5% for the five measurements.

Colorimetric sensor for pH. Once the change in the color intensity of Cdots with pH was observed, it is reasonable to use these properties to determine pH by measurement of color from images captured using a camera. By far, the most commonly used color space is RGB, the coordinates of which are used for processing with multivariate techniques. However, we used the

HSV color space in this work, whose main characteristic is that it represents useful information about the color in one single parameter, the *H* coordinate. Previous studies from our research group have shown that the use of *H* value is stable, simple to calculate, and easily obtained from commercial devices, maintaining superior precision with variations in reagents' colorimetric concentration, detector spectral response and illumination.[16]

As seen in Fig. 5A, the effect of pH on the color of Cdots is reflected by a shift from grey colors corresponding to acid pH values to yellow-orange color associated with medium pH values, and to brown color related to more basic pH values, which can also be easily observed by the naked eye. The relationship between the analytical parameter *H* and the pH was adjusted to a sigmoidal fit using a Boltzmann type equation, giving an apparent pK_a value of 6.7, which is in concordance with the acidic groups present on the surface of the Cdots.[17] As can be seen from both approaches, a wide linear range can be obtained from pH 3.5 to 10.2 (Fig. 5B).

Bioimaging and cytotoxicity. Fluorescence microscopy allowed us to examine the cellular localization of Cdots in HEK293 cells. Interestingly, we found that fluorescent Cdots were adsorbed on the cell membrane of HEK293 cells after a short incubation time (24 h) (right panel in Fig. 6A). Cells showed dot shaped localization of Cdots (red arrow, Fig. 6A) throughout cell bodies and did not reveal any impact of the Cdots on the cellular morphology. No evidence of fluorescence was observed in the control sample of untreated cells (data not
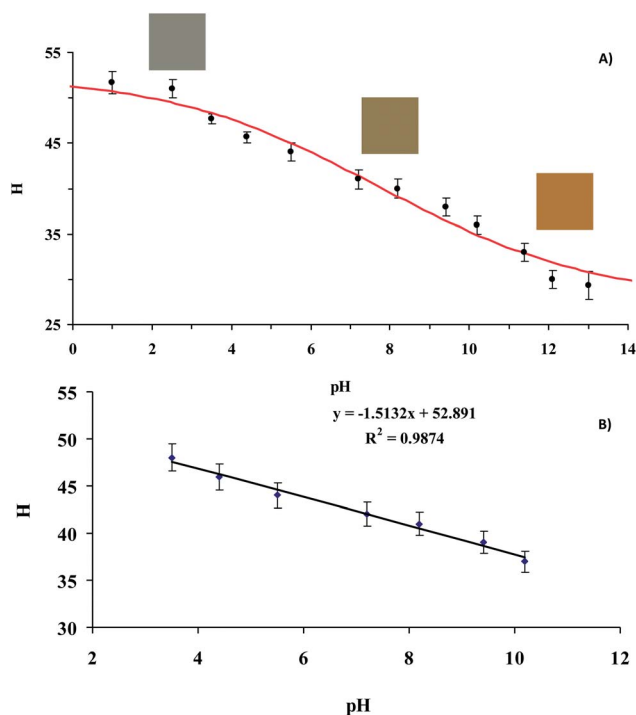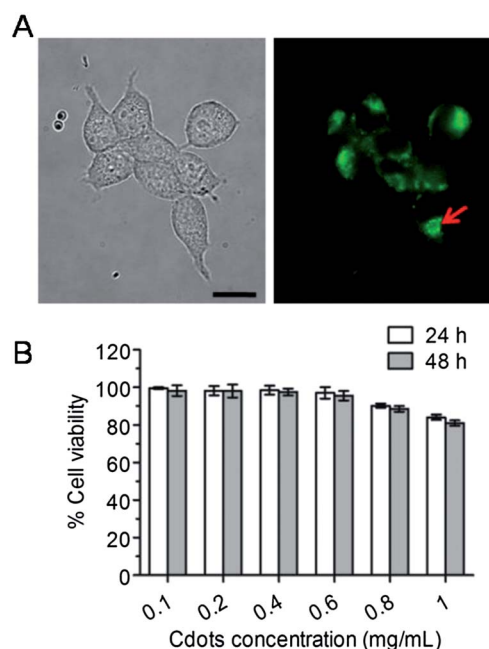

Fig. 6 Biological characterization of Cdots in HEK293 cells. (A) Transmitted light brightfield image of HEK293 cells (left panel) and fluorescence image showing in green the Cdots in the membrane edges and localized in small dots (red arrow). Scale bar = 10 μM. (B) MTT assay revealed no change in cell viability of HEK293 cells following a treatment with increasing concentrations of Cdots for 24 and 48 h at 37 °C.

Fig. 5 (A) Colorimetric response of Cdots in the pH range 1.5–13. (B) Linear range for pH colorimetric detection.

shown). As shown in Fig. 6B, cell viability was not affected in the presence of these concentrations of Cdots, demonstrating that these non-toxic nanoparticles can act as suitable biosensors or bioimaging devices in living organisms.

4. Conclusions

A microfluidic system has been proposed for the automatic synthesis of carbon dots. The system is composed of two separate platforms to increase its versatility, one for heating and control of the temperature and the other for microfluidics. The radial configuration of the heater as well as of the microfluidic pattern, which perfectly matches with the screen-printed resistor, permits a controlled mass and temperature transference. Once the hydrodynamic parameters of the microsystem were optimized, Cdots with suitable optical properties were obtained. The narrow size distribution observed in the characterization of the synthesized Cdots demonstrates the reproducibility of the microsystem. Further characterization of the synthesized Cdots showed the pH dependence of their optical properties which were used for the development of a pH fluorescent sensor using both UV and NIR excitation sources. The naked eye and a photographic digital camera were used as detection systems for the colorimetric pH measurement and were implemented using the H parameter, obtaining a linear response over a wide range of pH values. Cytotoxicity and permeability studies on cells did not reveal any impact on the cellular morphology. Viability of cells was not affected in the presence of different concentrations of Cdots, demonstrating their suitability for biosensing or bioimaging applications in the biomedical field.

Acknowledgements

Notes and references

1 (a) D. Mhamma, W. Ramadan, A. Rana, C. Rode, B. Hannuyer and S. Orgale, *Green Chem.*, 2011, **13**, 1990; (b) J. Ming, R. Liu, G. Liang, Y. Yu and F. Zhao, *J. Mater. Chem.*, 2011, **21**, 10929.
2 (a) K. Qu, J. Wang, J. Ren and Xi. Qu, *Chem.–Eur. J.*, 2013, **19**(22), 7243; (b) L. Zhou, Y. Lin, Z. Huang, J. Ren and X. Qu, *Chem. Commun.*, 2012, **48**(8), 1147.
3 (a) S. N. Baker and G. A. Baker, *Angew. Chem., Int. Ed.*, 2010, **49**, 2; (b) J. C. G. Estevez da Silva and H. M. R. Gonçalves, *Trends Anal. Chem.*, 2011, **30**, 1327; (c) S. K. Bhunia, A. Saha, A. R. Maity, S. C. Ray and N. R. Jana, *Sci. Rep.*, 2013, **3**, 1473; (d) H. Li, Z. Kang, Y. Liu and S. T. Lee, *J. Mater. Chem.*, 2012, **22**, 24230.
4 (a) H. Ming, Z. Ma, Y. Liu, K. Pan, H. Yu, F. Wang and Z. Kang, *Dalton Trans.*, 2012, **41**, 9526; (b) L. Zheng, Y. Chi, Y. Dong, J. Lin and B. Wang, *J. Am. Chem. Soc.*, 2009, **131**, 4564.
5 (a) X. Zhai, P. Zhang, C. Liu, J. Bai, W. Li, L. Dai and W. Liu, *Chem. Commun.*, 2012, **48**, 7955; (b) A. Salinas-Castillo, M. Ariza-Avidad, C. Pritz, M. Camprubí-Robles, B. Fernández, M. J. Ruedas-Rama, A. Megía-Fernández, A. Lapresta-Fernández, F. Santoyo-Gonzalez, A. Schrott-Fischer and L. F. Capitan-Vallvey, *Chem. Commun.*, 2013, **49**, 1103; (c) X. Jia, J. Li and E. Wang, *Nanoscale*, 2012, **4**, 5572.
6 (a) A. M. Nightingale, S. H. Krishnadasan, D. Berhanu, X. Niu, C. Drury, R. McIntyre, E. Valsami-Jones and J. C. deMello, *Lab Chip*, 2011, **11**, 1221; (b) H. Wang, X. Li, M. Uehara, Y. Yamaguchi, H. Nakamura, M. Miyazaki, H. Shimizu and H. Maeda, *Chem. Commun.*, 2004, 48; (c) E. M. Chan, A. P. Alivisatos and R. A. Mathies, *J. Am. Chem. Soc.*, 2005, **127**, 13854.
7 (a) S. Gomez-de Pedro, M. Puyol, D. Izquierdo, I. Salinas, J. M. de la Fuente and J. Alonso-Chamarro, *Nanoscale*, 2012, **4**(4), 1328; (b) S. Gomez de Pedro, M. Puyol and J. Alonso, *Nanotechnol.*, 2010, **21**(41), 415603.
8 (a) C. S. Martinez-Cisneros, Z. daRocha, M. Ferreira, F. Valdes, A. Seabra, M. Gongora-Rubio and J. Alonso-Chamarro, *Anal. Chem.*, 2009, **81**, 7448; (b) G. Fercher, A. Haller, W. Smetana and M. J. Vellekoop, *Analyst*, 2010, **135**, 965.
9 S. Gómez-de Pedro, C. S. Martínez-Cisneros, M. Puyol and J. Alonso-Chamarro, *Lab Chip*, 2012, **12**, 1979.
10 N. Ibáñez-García, C. S. Martínez-Cisneros, F. Valdés and J. Alonso, *TrAC, Trends Anal. Chem.*, 2008, **27**, 24.
11 C. S. Martínez-Cisneros, S. Gómez-de Pedro, J. García-García, M. Puyol and J. Alonso-Chamarro, *Chem. Eng. J.*, 2012, **211–212**, 432.
12 F. C. Thyrion and G. Debecker, *Int. J. Chem. Kinet.*, 1973, **5**, 583.
13 B. K. H. Yen, N. E. Stott, K. F. Jensen and M. G. Bawendi, *Adv. Mater.*, 2003, **15**, 1858.
14 L. Tian, D. Ghosh, W. Chen, S. Pradhan, X. Chang and S. Chen, *Chem. Mater.*, 2009, **21**, 2803.
15 (a) J. L. Chen and X. P. Yan, *Chem. Commun.*, 2011, **47**, 3135; (b) W. Kong, H. Wu, Z. Ye, R. Li, T. Xu and B. Zhang, *J. Lumin.*, 2014, **148**, 238.
16 (a) K. Cantrell, M. M. Erenas, I. De Orbe-Payá and L. F. Capitán-Vallvey, *Anal. Chem.*, 2010, **82**, 531; (b) M. Ariza-Avidad, M. P. Cuellar, A. Salinas-Castillo, M. C. Pegalajar, J. Vukovic and L. F. Capitán-Vallvey, *Anal. Chim. Acta*, 2013, **783**, 56.
17 A. Lapresta-Fernández and L. F. Capitán-Vallvey, *Anal. Chim. Acta*, 2011, **706**, 328.